ACS OMEGA

http://pubs.acs.org/journal/acsodf

Article

Rich D-Fructose-Containing Polysaccharide Isolated from *Myxopyrum smilacifolium* Roots toward a Superior Antioxidant Biomaterial

Trung Hieu Le,* Lam Son Le, Dang Giang Chau Nguyen, Thi Van Thi Tran, Xuan Anh Vu Ho, Thanh Minh Tran, Minh Nhung Nguyen, Viet Thang Nguyen, Thuy Trang Le, Thi Hong Chuong Nguyen, Chinh Chien Nguyen,* and Quyet Van Le*

Cite This: *ACS Omega* 2022, 7, 47923−47932

Read Online

ACCESS | Metrics & More | Article Recommendations | Supporting Information

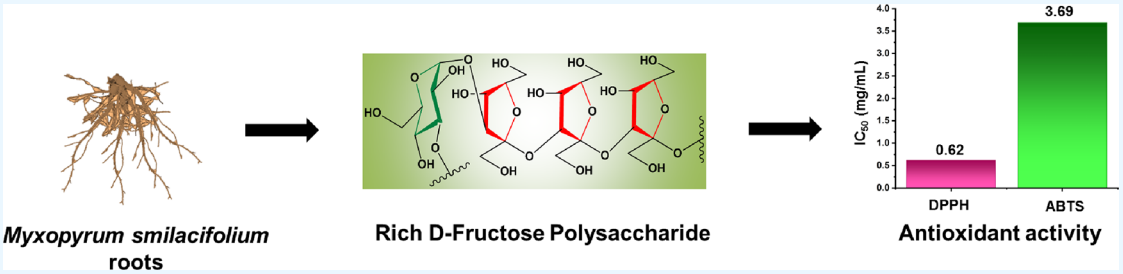

ABSTRACT: The presented study attempts to unveil and evaluate the antioxidant activity of a novel heteropolysaccharide separated from the roots of *Myxopyrum smilacifolium* (denoted as PS-MSR). The molecular weight of PS-MSR is found to be 1.88×10^4 Da and contains two principal sugars, which are D-glucose and D-fructose, in the backbone. Decoding the structure of the obtained PS-MSR sample has disclosed a novel polysaccharide for the first time. Indeed, the PS-MSR is composed of (1 → 3)-linked glucosyl units and (2 → 3)-linked fructosyl units. In addition, the 1D and 2D NMR spectra of the PS-MSR sample display the repeating unit of the isolated polysaccharide, [→3)-*α*-D-Glc*p*-(1 → 3)-*β*-D-Fruc*f*-(2 → 3)-*β*-D-Fruc*f*-2 → 3)-)-*β*-D-Fruc*f*-*β*-(2→]$_n$. Interestingly, the PS-MSR sample exhibits outstanding antioxidant activity, signifying the potential utilization of the explored polysaccharide for antioxidant-based material.

1. INTRODUCTION

Polysaccharides (PSs) have attracted great interest due to their noble biological activities (e.g., antioxidant, antiangiogenic, antiviral, and anticancer).[1−10] In addition, PSs have exhibited notable capability for inhibiting lipid peroxidation, antiaging, hypoglycemic effects, and immunoregulation.[11−13] Hence, PS utilization has arisen as a promising approach to tackle and/or support the treatment of hotspot diseases.[2,7,8]

As a proof of concept, the polysaccharides have usually been found as a linear structure containing sugar residues, forming monosaccharides and oligosaccharides connected via glycosidic bonds.[14−16] Also, inter- and intra-chain hydrogen bonding are also found. To this end, the sugar residues (i.e., D-glucose and D-fructose) have been considered the primary factor, significantly contributing to the biological activity outcomes.[17,18] In other words, the arrangement and amount of each component could drive the bioactivity outcomes.

Hitherto, numerous various PS structures have been explored over the past decades. It turns out that the obtained PS structures are widely varied, depending on the investigated natural sources.[1,19−21] Moreover, the composition of D-glucose is found to be the dominant constituent, whereas D-fructose in the explored PS backbone is rarely reported. As a result, foraging the novel natural sources possessing rich D-fructose has been considered the priority approach to address the mentioned issue.

Myxopyrum smilacifolium, a member of the Oleaceae family in Asian south-eastern tropical and subtropical regions, has been considered an essential medicinal plant proven to be efficient for cough, rheumatism, nerve complaints, asthma, fever, neuropathy, and asthma treatments.[22−24] *M. smilacifolium* extracts exhibited noble biological activities (e.g., antimicrobial, cytotoxic, anti-inflammatory, and antioxidant activities).[23−26] Nevertheless, the reason for inducing the bioactivities of *M. smilacifolium* has been ambiguous. Given this, polysaccharides could be the primary component of *M. smilacifolium* extracts,

Received: September 6, 2022
Accepted: December 1, 2022
Published: December 13, 2022

https://doi.org/10.1021/acsomega.2c05779
ACS Omega 2022, 7, 47923−47932

Scheme 1. Schematic Illustration of the Antioxidant Activity of PS-MSR

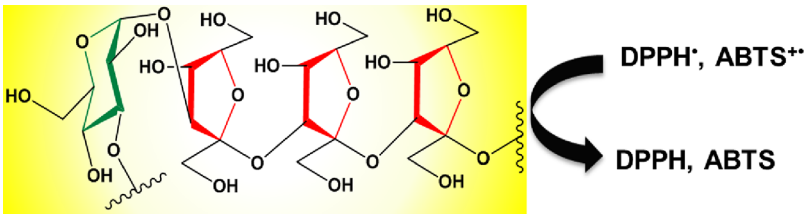

causing the antioxidant activity. In this context, the polysaccharide structure can be considered the imperative piece of information explaining their outstanding bioactivities. Unfortunately, the structural and bioactive properties of purified PS extracted from the roots of *M. smilacifolium* are rarely reported. Therefore, decoding the structure and evaluating the antioxidant activities of *M. smilacifoliu*-derived water-soluble polysaccharides are highly urgent.

Herein, we report a structural study on polysaccharides from the roots of *M. smilacifolium* (denoted as PS-MSR). Impressively, utilizing advanced characterization techniques to identify the PS structure, we explore a novel and rich D-fructose PS, which is [→3)-*α*-D-Glc*p*-(1 → 3)-*β*-D-Fruc*f*-(2 → 3))-*β*-D-Fruc*f*-2 → 3)-)-*β*-D-Fruc*f*-*β*-(2→]$_n$, for the first time. Indeed, the composition of D-fructose is found to be dominant, which is rarely found elsewhere. Such features resulted in outstanding *in vitro* antioxidant activities, suggesting that the obtained PS-MSR could function as a natural antioxidant. This new discovery further fulfills the database of PSs isolated from the roots of *M. smilacifolium* and discloses bright prospects in biomedical applications.

2. EXPERIMENTAL SECTION

2.1. Materials. The *M. smilacifolium* roots were collected from a natural source in June 10th, 2021, in Thua Thien Hue, Vietnam. The identification and voucher specimen were conducted and deposited at the Department of Biology, College of Sciences, Hue University.

2.2. Chemicals. Diethylaminoethyl cellulose-52 and dialysis membranes (M_w cut-off 8000−14,000 Da) were supplied by Thermo Fisher. Gallic acid, ascorbic acid Sephadex G-100, $(CH_3)_2SO$, $(CH_3)_2SO_4$, $NaBH_4$, and 2,2-diphenyl-1-picrylhydrazyl (DPPH) were supplied by Sigma-Aldrich.

2.3. Extraction and Purification of Polysaccharides. *2.3.1. Extraction of PS.* The water-soluble polysaccharides were collected through a two-step extraction, as shown in Scheme 2.[27] Briefly, the defatted *M. smilacifolium* root powder (50 g) was dried and subjected to ethanol 96% (1000 mL) at 78 °C for 3 h with three replicates to remove the decolorization, low-weight molecules. The residue was collected before being added into distilled water (1500 mL) at 100 °C for 3 h to redissolve polysaccharides. The insoluble solid was discarded through centrifugation. The remaining solution was evaporated by the vacuum evaporator at 60 °C to remove water. Then, the concentrated extract solution was added into ethanol 96% according to a volume ratio of 1−4 to completely reprecipitate polysaccharides before being frozen at −10 °C for 24 h. The obtained precipitation was washed with cold ethanol followed by acetone twice and dried at 40 °C under vacuum to yield crude PS powder.

2.3.2. Purification of PS. The obtained PS powder, which was dissolved in water and dialyzed before being evaporated into a concentrated solution, was deproteinated through the Sevag method[28] before undergoing an anion-exchange process (diethylaminoethyl cellulose-52, 26 mm × 500 mm) using five different concentrations of NaCl solution (i.e., 0.0, 0.1, 0.3, 0.5, and 1.0 M) at a flow rate of 1 mL/min. The phenol−sulfuric acid method was utilized to screen each fraction.[29] The fractions were named Fractions I−V, corresponding to each concentration of NaCl solution. It turns out that Fraction I, which contained the highest amount of neutral carbohydrates (96%), was concentrated, lyophilized, and purified on a Sephadex G-100 column (10 mm × 600 mm) before being eluted with deionized water, NaCl 0.1 M, and NaCl 0.3 M eluents (flow rate, 0.2 mL/min), respectively. Finally, the achieved PS was obtained for further investigations.[30,31]

2.4. Determination of Molecular Mass. Gel permeation chromatography (Agilent 1100 Series coupled to an MS detector, microTOF-QII Bruker) was carried out to determine the average molecular weight (M_w), number average molecular weight (M_n), and polydispersity index (M_w/M_n) of PS.[32] In a typical experiment, the 0.1 mol/L $NaNO_3$ solution (10 μL) was added to dissolve the purified PS before being injected into the system. The column (Ultrahydrogen 500; 7.8 mm × 300 mm, 10 μm) was eluted with the 0.1 mol/L $NaNO_3$ solutions containing 0.1 g/L NaN_3 at 40 °C at a flow rate of 1 mL/min. Calibration was conducted with standard series pullulan (M_w of 5, 20, 100, 200, 400, and 800 kDa).

2.5. Monosaccharide Composition and Methylation Analysis. The polysaccharide samples were methylated using the mixture of $(CH_3)_2SO_4$ and solid NaOH for 16 h in $(CH_3)_2SO$ at 60 °C. As completed, methylated PS (50 mg) was hydrolyzed by trifluoroacetic acid 2 M (4 mL) for 2 h at 120 °C followed by the sample enrichment under the stream of N_2. Then, methanol was introduced to remove the excess TFA through co-evaporation under N_2 flow. A solution of $NaBH_4$ (0.25 M) in NH_3 was introduced into the leftover methylated monosaccharides for the reduction at room temperature. The solution was then neutralized by CH_3COOH 10% in CH_3OH (5 mL) and underwent co-evaporation with CH_3OH under N_2 flow to remove the excess acid. The obtained sample was subjected to 2 mL of solution of anhydride acetic and pyridine (1.1, v/v) at 100 °C for 20 min and dried under a N_2 stream. The final product was redissolved in $CHCl_3$ for GC−MS analysis.[33−37]

2.6. GC−MS Analysis. The GS-MS program was set as follows: the carrier gas, He; pressure, 15 psi; injected volume, 1 μL; split ratio, 10:1; and the injection temperature, 250 °C. The temperature program was 150 °C, 10 °C/min to 280 °C for 5 min. The MS source condition was set as follows: ionization energy, 70 eV; interface temperature, 280 °C; MS temperature, 230 °C; and quadrupole temperature, 150 °C.

2.7. Infrared Spectroscopy Analysis. The mixture of the dried PS powder (2 mg) and KBr powder was ground and pressed into 1 mm-thick pellets. The as-prepared sample was conducted by an infrared spectrophotometer (IRPrestige-21).

https://doi.org/10.1021/acsomega.2c05779
ACS Omega 2022, 7, 47923−47932

Scheme 2. Schematic Illustration of the Extraction and Purification of *M. smilacifolium* Polysaccharide

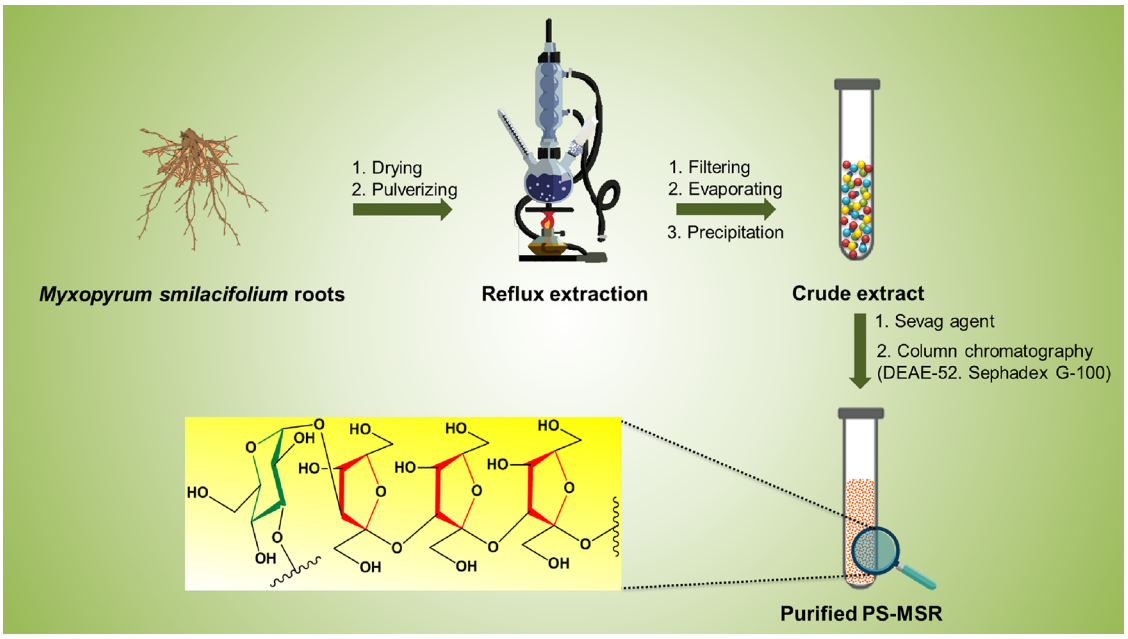

The scan range was from 4000 to 400 cm^{-1} with a resolution of 8 cm^{-1}.

2.8. NMR Method. D_2O (1 mL) was used to dissolve the pattern powder (10 mg) for NMR analysis (Bruker Avance 500 Hz spectrometer) at 302.5 and 302.9 K. Trimethylsilane (TMS) was utilized as an internal reference. Chemical shifts (δ) were given in parts per million (ppm).

2.9. *In Vitro* Antioxidant Activity Evaluation. Free radical scavenging, driven by lipid oxidation inhibition mechanisms, has been considered an outstanding approach to evaluate antioxidant activity. In this study, ABTS radical scavenging and DPPH free radical scavenging methods were employed to precisely determine the antioxidant activity of extracted polysaccharide samples through their ability to donate hydrogen atoms, as depicted in Scheme 1.

2.9.1. Total Antioxidant Activity. The total antioxidant capability was assessed by using the phospho-molybdenum method.[38,39] Briefly, the sample (0.3 mL) was added to 3 mL of a reagent solution consisting of sulfuric acid (0.6 M), sodium phosphate (28 mM), and ammonium molybdate (4 mM) before being incubated at 95 °C for 90 min. After cooling to 25 °C, the obtained solution was measured at a wavelength of 695 nm. The blank sample was prepared by a similar procedure without the sample. The standard curve equations of gallic acid and ascorbic acid with concentrations from 0.1 to 0.5 mg/mL were found to be $Y = 2.172 \times X_{GA} + 0.1056$, $R = 0.9995$ and $Y = 4.209 \times X_{AS} - 0.0463$, $R = 0.9993$, respectively.

2.9.2. ABTS Radical Scavenging Assay. ABTS (7 mM) with potassium persulfate (2.45 mM) was placed in the dark at room temperature for 16 h to produce the ABTS radical.[40] The sample (0.1 mL) possessing the concentration range from 1 to 5 mg/mL was dissolved with $ABTS^{+\cdot}$ solution (3.9 mL) and measured at 734 nm. Ascorbic acid was utilized as a positive control. The scavenging capability toward $ABTS^{+\cdot}$ was calculated as follows: scavenging rate (%) = $[1 - OD_{sample}/OD_{blank}] \times 100$.

The IC_{50} value was used to evaluate the radical scavenging activity.

2.9.3. Evaluation of DPPH Radical Scavenging Activity. The extract (2 mL) corresponding to the concentration range of 0.4−2 mg/mL was added to 100 μM DPPH in ethanol (1 mL). The homogeneous solution was incubated for 30 min at ambient temperature before being measured at optical density (OD) at a wavelength of 517 nm (Jasco V-630 spectrophotometer).[41] Ascorbic acid was used as a positive control with concentrations from 2 to 10 μg/mL. Ethanol was employed as a blank sample. The scavenging activity was calculated according to the formula as follows:

$$\text{scavenging rate (\%)} = [1 - (OD_{sample} - OD_{control\ sample})/OD_{blank}] \times 100$$

where OD_{blank}, OD_{sample}, and $OD_{control\ sample}$ are the absorbances of the blank sample, polysaccharide sample, and control sample, respectively. The radical scavenging activity was assessed through the IC_{50} value.

2.10. Statistical Analysis. The experiments were carried out three times ($n = 3$). The data were presented as mean value ± standard deviation (SD) (or standard error of the mean (SEM)). One-way ANOVA was used to determine the subjecting to an analysis of variances. The mean value of $p < 0.05$ was statistically significant.

3. RESULTS AND DISCUSSION

3.1. Characterizations of Obtained Polysaccharides. Scheme 2 illustrates the extraction and purification of *M. smilacifolium* polysaccharide, employing dissolved and reprecipitated polysaccharide in water and ethanol, respectively. In this circumstance, the polarity of the solvent is the primary. Polysaccharides contain not only free −OH groups but also −COOH groups, so they are polar compounds. Therefore, most polysaccharides are insoluble in less polar and moderately polar solvents such as acetone, *n*-hexane, benzene, ethyl acetate, tetrachloromethane, chloroform, ether petroleum, and ethanol but soluble in polar solvents such as water, NaOH solution, etc. The polysaccharide content was determined by

https://doi.org/10.1021/acsomega.2c05779
ACS Omega 2022, 7, 47923−47932

employing the phenol-sulfuric acid colorimetric method with D-glucose as a standard at a wavelength of 490 nm.[29] The extraction yield of PS was 4.53 ± 0.05%.

Gel permeation high-performance liquid chromatography (GPHPLC) is employed to determine the average molecular weight of PS-MSR (see Section 2.4), as shown in Figure 1A.

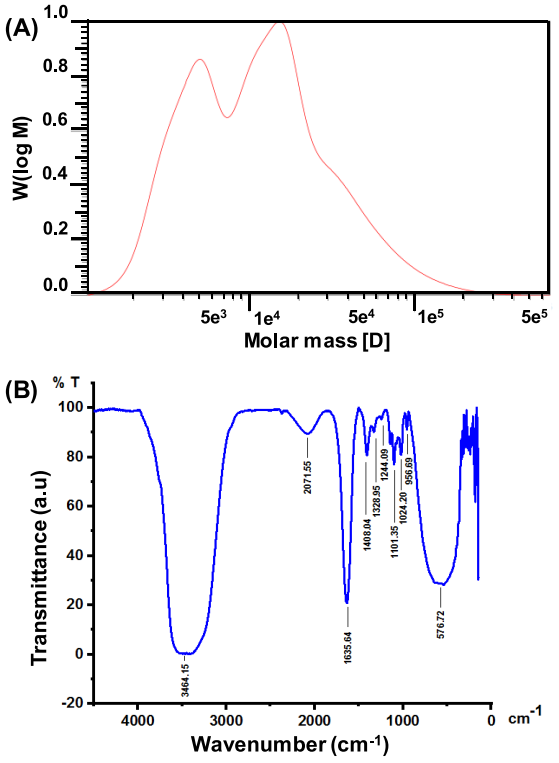

Figure 1. Molecular mass chromatogram (A) and the IR spectrum (B) of PS-MSR from *M. smilacifolium*.

Two peaks centering at 6.84×10^3 and 2.13×10^4 Da could be distinguished. To this end, the average molecular weight of PS-MSR is ~1.88×10^4 Da. The M_w/M_n ratio is found to be ~1.30, implying a large molecular weight distribution, suggesting the heterogeneous feature of the obtained PS-MSR.

Fourier-transform infrared spectroscopy (FT-IR) was conducted to investigate the characteristic bonding of the sample PS-MSR, as shown in Figure 1B. The intense and broad peak centering at 3464 cm^{-1} could be attributed to the O−H stretching vibration.[42−45] The characteristic peak centering at 1143 cm^{-1} implies a glucopyranoside, whereas the peaks located at 1024 and 956 cm^{-1} could be ascribed to α-configurations and the presence of fructose residues, respectively.[44] To this end, it can be said that the extracted PS-MSR sample possesses the typical absorption groups of polysaccharides and fructose in the structure.

3.1.1. Methylation Analysis. Gas chromatography−mass spectrometry (GC−MS) analysis was carried out to investigate the composition and interglycosidic linkages between monosaccharide residues of the as-obtained PS-MSR sample. GC−MS chromatography, using the NIST14 database, indicates two crucial peaks at retention times of 19.213 and 21.026 min, respectively, corresponding to two main methylated sugar derivatives, 1,3,5-tri-*O*-acetyl-2,4,6-tri-*O*-methylglucitol and 2,3,5-tri-*O*-acetyl-1,4,6-tri-*O*-methylfructitol, as shown in Figure S1. This signifies the attendance of D-glucose and D-fructose in the backbone. Moreover, GC−MS results also prove the attendance of 3-*O*-substituted Glc*p* and 3-*O*-substituted Fru*f* in the obtained polysaccharide structure, which suggests a repeating linear disaccharide with glucose units in the pyranose ring form and fructose units in the furanose ring form. Therefore, two types of linkages, (1 → 3)-linked glucosyl and (2 → 3)-linked fructosyl, are present in the PS-MSR. Impressively, the D-fructose component accounts for the high content in the structure of polysaccharides.

Table 1. Correlations Involving Atoms Observed in the HBMC and COSY Spectra of PS-MSR from *M. smilacifolium* Recorded in D_2O

sugar residue	sugar linkage	HMBC ($^1H \rightarrow ^{13}C$)	COSY ($^1H \rightarrow ^1H$)
A	→3)-α-D-glucopyranoside-(1→	H-1 (δ 5.41)/C-2 (δ 72.6)	H-2 (δ 3.72)/H-3 (δ 3.50)
		H-2 (δ 3.72)/C-3 (δ 72.1)	H-3 (δ 3.50)/H-2 (δ 3.72)/H-4 (δ 3.82)
		H-3 (δ 3.72)/C-4 (δ 72.5)/C-2 (δ 72.6)	H-4 (δ 3.82)/H-3 (δ 3.50)/H-5 (δ 4.06)
		H-4 (δ 3.82)/C-3 (δ 71.2)/C-5 (δ 74.5)	H-5 (δ 3.81)/H-4 (δ 3.82)/H-6 (δ 3.75)
		H-5 (δ 4.06)/C-4 (δ 72.5)/C-6 (δ 62.3)	
B	→3)-β-D-frucofuranoside-(2→	H-1 (δ 3.72)/C-2 (δ 103.3)	H-4 (δ 4.23)/H-3 (δ 3.68)/H-5 (δ 3.74)
		H-3 (δ 3.68)/C-2 (δ 103.3)/C-4 (δ 76.9)	H-5 (δ 3.74)/H-4 (δ 4.23)/H-6 (δ 3.78)
		H-4 (δ 4.23)/C-3 (δ 60.5)/C-5 (δ 81.1)	
		H-5 (δ 3.68)/C-4 (δ 76.9)/C-6 (δ 62.2)	
C	→3)-β-D-frucofuranoside-(2→	H-1 (δ 3.80)/C-2 (δ 103.1)	H-4 (δ 4.14)/H-3 (δ 3.69)/H-5 (δ 4.16)
		H-3 (δ 3.69)/C-2 (δ 103.1)/C-4 (δ 76.8)	H-5 (δ 4.16)/H-4 (δ 4.14)/H-6 (δ 3.73)
		H-4 (δ 4.14)/C-3 (δ 60.9)/C-5 (δ 74.4)	
		H-5 (δ 4.16)/C-4 (δ 76.8) C-6 (δ 60.2)	
D	→3)-β-D-frucofuranoside-(2→	H-1 (δ 4.01)/C-2 (δ 103.7)	H-4 (δ 4.20)/H-3 (δ 3.82)/H-5 (δ 3.85)
		H-3 (δ 3.82)/C-2 (δ 103.7)/C-4 (δ 77.6)	H-5 (δ 3.85)/H-4 (δ 4.20)/H-6 (δ 3.44)
		H-4 (δ 4.20)/C-3 (δ 61.1)/C-5 (δ 81.3)	
		H-5 (δ 4.16)/C-4 (δ 77.6)/C-6 (δ 69.3)	

3.1.2. 1D and 2D NMR Spectroscopy Analysis of PS-MSR. The 1D and 2D nuclear magnetic resonances (NMR) were employed to provide an in-depth and sufficient order of D-glucose and D-fructose within the polysaccharide structure. As shown in the ^1H spectrum (Figure 2A), sugar protons can be recognized in the region of 3.44−4.23 ppm. The signal appearing at δ 5.41 (d, $J_{H\text{-}1,H\text{-}2}$ = 4 Hz) ppm in the anomeric region originated from H-1 of the α-D-glucopyranosyl residue. Figure 2B displays the ^{13}C NMR spectrum of the PS-MSR sample, providing two essential data in the structure of the polysaccharide, as follows: (i) the signal emerging at δ 92.5 ppm is assigned to C-1 of α-D-glucopyranosyl residues; (ii) the peaks centering at chemical shift values of 103.1, 103.3, and 103.7 ppm in the anomeric carbon region could be attributed to C-2 of fructose. Particularly, the signal centering at 103.1 ppm is the typical peak of β-(1 → 3)-linkaged D-fructose. The signals located at 103.3 and 103.7 ppm can be ascribed to a β-(2 → 3)-linked D-fructosyl residue. To this end, 1D NMR data

https://doi.org/10.1021/acsomega.2c05779
ACS Omega 2022, 7, 47923−47932

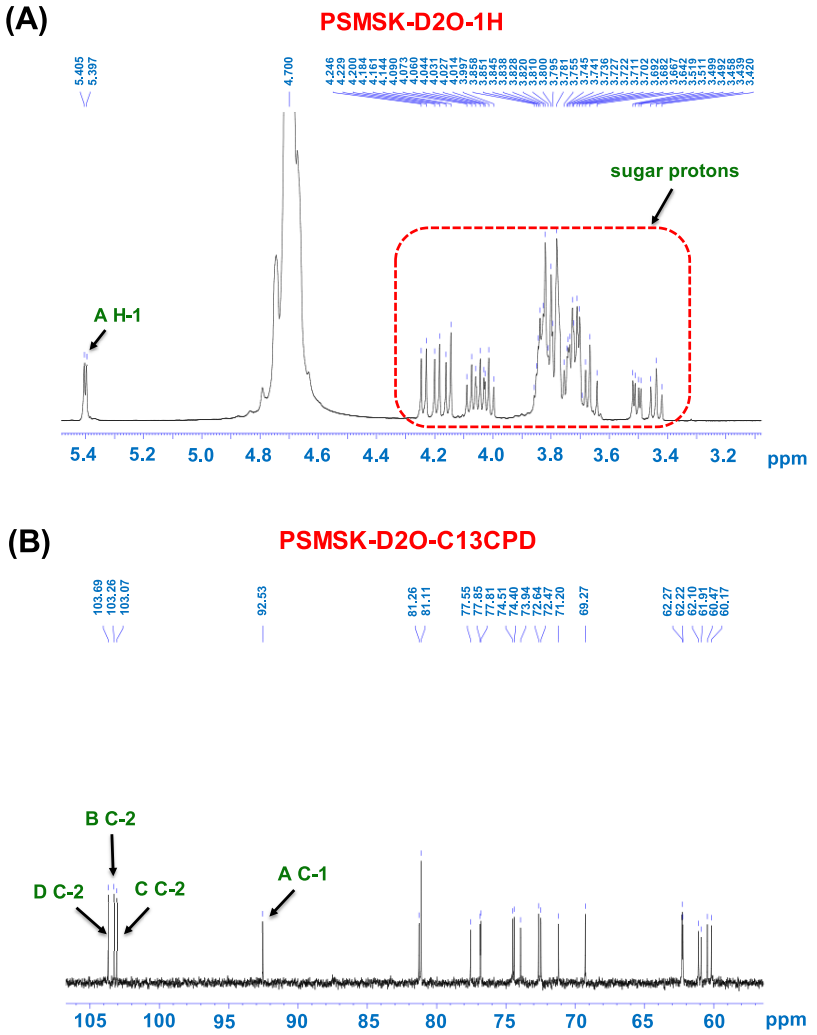

Figure 2. 1D NMR spectrum of PS-MSR: (A) ^{1}H NMR; (B) ^{13}C NMR.

verify the existence of D-glucose and D-fructose in the repeating unit of PS-MSR.

The 2D NMR technique was utilized to characterize the detailed chemical structure of PS-MSR. The ^{1}H−^{13}C HSQC spectrum (Figure 3A,B) exhibits cross-peaks in the region for anomeric resonances δ_C 60.2−103.7 ppm and δ_H 3.44−5.41 ppm. In this circumstance, the signals centering at δ 5.41/92.5, δ 3.72/72.6, δ 3.50/71.2, δ 3.82/72.5, δ 4.06/74.5, and δ 3.75/62.3 imply residue A. In addition, the signals found at δ 3.72/60.9, δ 3.68/60.5, δ 4.23/76.9, δ 3.74/81.1, and δ 3.78/62.2 confirm sugar residue B. The signals positioning at δ 3.80/72.5, δ 3.69/60.9, δ 4.14/76.8, δ 4.16/74.4, and δ 3.73/60.2 indicate residue C, while residue D was associated with the signals at δ 4.01/73.9, δ 3.82/61.1, δ 4.20/77.6, δ 3.85/81.3, and δ 3.44/69.3. The achieved 2D NMR result indicates the positions within each sugar residue, which are suggested by the downfield chemical shifts of the ^{1}H and ^{13}C resonances.

The correlations in the heteronuclear multiple bond correlation (HMBC) and correlated spectroscopy (COSY) NMR were investigated to identify the positions of H-1−6 and C-1−6 of sugar residues, as shown in Figures 3 and 4. The HMBC spectrum-derived interactions from ^{1}H → ^{13}C show the interaction between protons and adjacent carbon, as shown in Table 1. Such results reveal the bonding order of hydrogen and carbon in the sugar components of the PS-MSR: →3)-*α*-D-glucopyranoside-(1→; →3)-*β*-D-frucofuranoside-(1,→3)-*β*-D-frucofuranoside-(1→,→3)-*β*-D-frucofuranoside-(1→.

The ^{1}H−^{1}H COSY spectra of sugar A, B, C, and D residues offer interactions between protons in sugar units, as shown in Figure 4A,B. To this point, the detailed correlations can be identified, as shown in Table 1. Such data unveils the carbon linkage sequence of the monosaccharides in the PS-MSR structure as →3)-*α*-D-glucopyranoside-(1→;→3)-*β*-D-frucofuranoside-(2→;→3)-*β*-D-frucofuranoside-(2→;→3)-*β*-D-frucofuranoside-(2→. On the basis of obtained characterization results, the chemical bonding details of the *M. smilacifolium* polysaccharide are pointed out, as shown in Table 2.

The sugar chain of the PS-MSR structure can be determined via the HMBC and NOESY spectra. The inter-residue cross-linkings in the HMBC spectrum between the protons and the carbons at the linkages between A H-1 and B C-3, C H-3 and B C-2, and D H-3 and C C-3. Additionally, the NOESY spectrum showed strong correlations between A H-1/B H-3, between C H-3/B H-1/B H-5, and between D H-3/C H-1/C H-5 (Figure 4C). These linkages confirmed the attendance of A(1 → 3)B, B(2 → 3)C, and C(2 → 3)D bonding, which is consistent with the GC−MS outcome. The obtained polysaccharide can be decoded as [→3)-*α*-D-Glc*p*-(1 → 3)-*β*-D-Fruc*f*-(2 → 3))-*β*-D-Fruc*f*-2 → 3)-)-*β*-D-Fruc*f*-*β*-(2→]$_n$. Impressively, the structure possesses rich D-Fruc*f*, which is

https://doi.org/10.1021/acsomega.2c05779
ACS Omega 2022, 7, 47923−47932

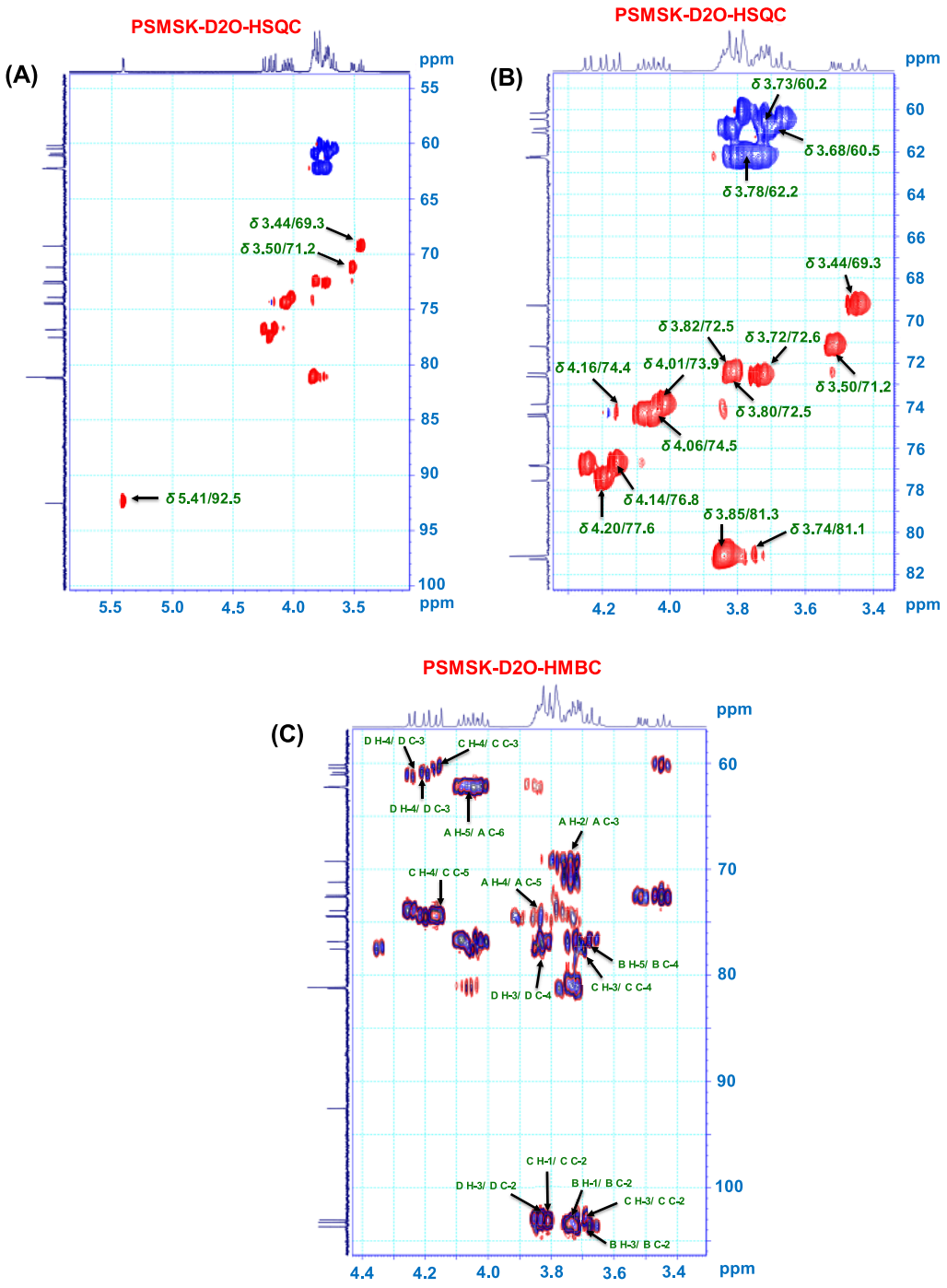

Figure 3. Overall (A) and expansion (B) of the 2D $^{1}H-^{13}C$ heteronuclear single-quantum correlation spectroscopy (HSQC) spectrum; (C) HMBC spectrum of PS-MSR.

rarely reported elsewhere. For the first time, a novel and rich D-Fruc*f* polysaccharide obtained from *M. smilacifolium* is explored, as shown in Figure 4D.

3.2. Antioxidant Activity Assay. The antioxidant capability was performed to evaluate the potential applications of the as-discovered *M. smilacifolium*-isolated polysaccharide, as shown in Figure 5 (see Scheme 1 in Section 2.9 for experimental details). The *in vitro* total antioxidant capability of the PS-MSR is found to be 0.2435 ± 0.0031 mg of GA/g or 0.2182 ± 0.0034 μmol of AS/g at a concentration of 1.5 mg/mL, suggesting the outstanding antioxidant capacity of the obtained PS-MSR sample.

ABTS radical scavenging activity of PS-MSR, considered one of the mechanisms that inhibit lipid oxidation, was also performed to estimate antioxidant activity, as depicted in Figure 5. The $ABTS^{+\cdot}$ scavenging activities of PS-MSR rise along with the increasing concentration and scavenging rate of PS-MSR. Indeed, the $ABTS^{+\cdot}$ scavenging activities are 20.76, 32.14, 43.28, 53.6, and 63.17%, corresponding to concentrations of 1−5 mg/mL, respectively. At a concentration of 5 mg/mL, the ABTS radical scavenging capacity of PS-MSR of *M. smilacifolium* was over 63%, but the activity of PS-MSR was lower than that of ascorbic acid. The ABTS radical scavenging activity of the presented polysaccharides is higher than that of

https://doi.org/10.1021/acsomega.2c05779
ACS Omega 2022, 7, 47923−47932

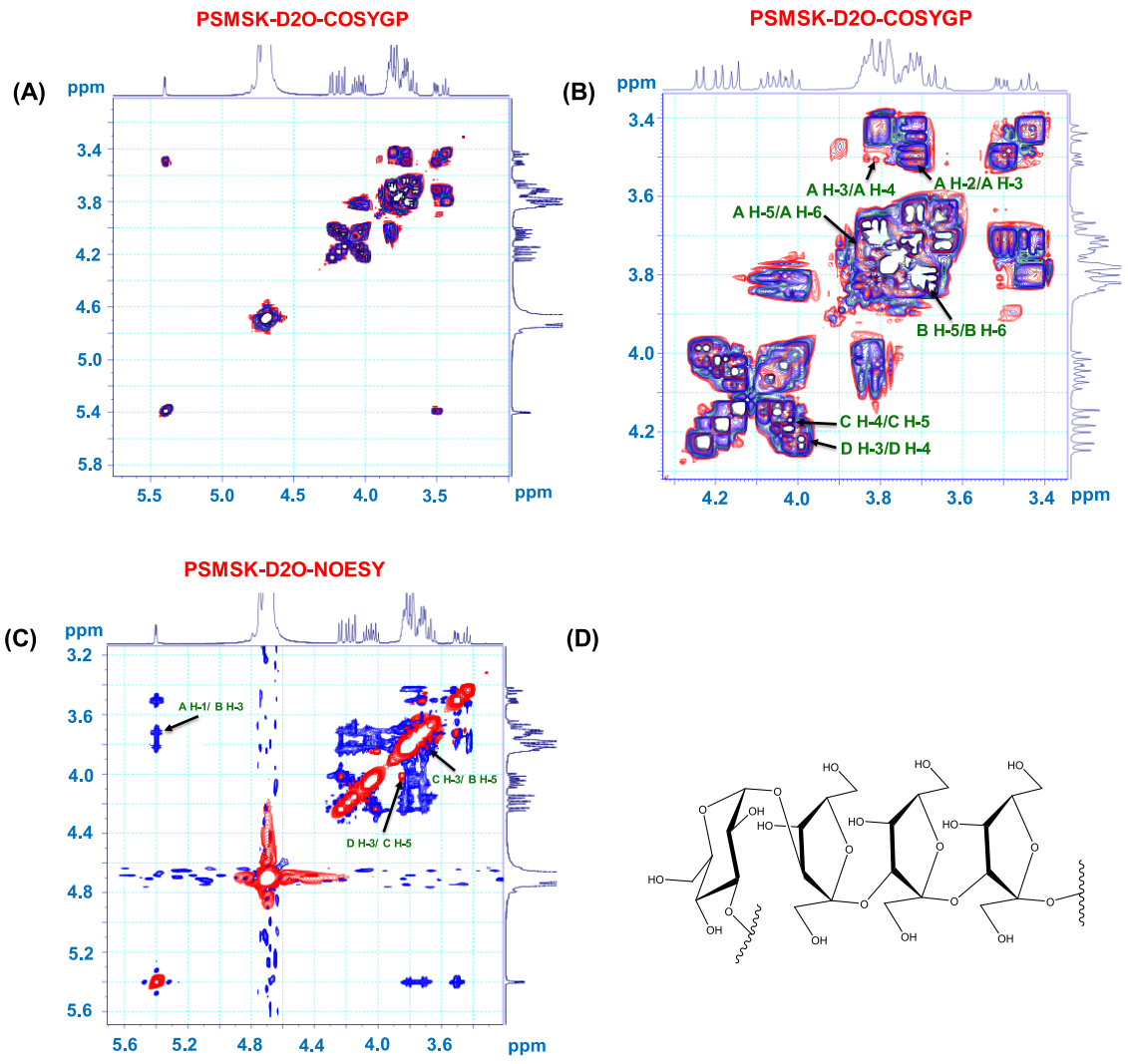

Figure 4. Overall (A) and expansion (B) of the $^{1}H-^{1}H$ COSY spectrum; $^{1}H-^{1}H$ NOESY spectrum (C); unveiling the structure of the repeating units (D) of PS-MSR from *M. smilacifolium*.

Table 2. NMR Chemical Shifts (δ, ppm) of PS from *M. smilacifolium* Recorded in D_2O

	sugar residue	H-1	H-2	H-3	H-4	H-5	H-6
A	→3)-α-D-glucopyranoside-(1→	5.41	3.72	3.50	3.82	4.06	3.75
B	→3)- β-D-frucofuranoside-(2→	3.72		3.68	4.23	3.74	3.78
C	→3)- β-D-frucofuranoside-(2→	3.80		3.69	4.14	4.16	3.73
D	→3)- β-D--frucofuranoside-(2→	4.01		3.82	4.20	3.85	3.44
	sugar residue	C-1	C-2	C-3	C-4	C-5	C-6
A	→3)-α-D-glucopyranoside-(1→	92.5	72.6	71.2	72.5	74.5	62.3
B	→3)-β-D-frucofuranoside-(1→	60.9	103.3	60.5	76.9	81.1	62.2
C	→3)-β-D-frucofuranoside-(1→	72.5	103.1	60.9	76.8	74.4	60.2
D	→3)-β-D-frucofuranoside-(1→	73.9	103.7	61.1	77.6	81.3	69.3

both *Ophiocordyceps sobolifera* polysaccharides (IC_{50}: 4.83 mg/mL).[46] Furthermore, the achieved IC_{50} value, 3.69 mg/mL, considerably outperforms those of variously reported polysaccharides, as shown in Table S1.

The DPPH radical scavenging test is also conducted to study the activity of antioxidants quantifying and comparing the free radical scavenging capabilities of various antioxidants. The antioxidant capacity of the PS-MSR of *M. smilacifolium* was evaluated with the DPPH method. The values of DPPH radical scavenging activity are depicted in Figure 5. The scavenging rates increase from 18.24 to 82.62%, corresponding to concentrations ranging from 0.4 to 2.0 mg/mL. The IC_{50} value of polysaccharides is found to be 0.62 mg/mL, which is found to be considerably higher than that of the reported polysaccharide, as depicted in Table S2. It turns out that the DPPH radical scavenging activities of the PS-MSR are also comparable to those of reported medicinal fungi. The DPPH radical scavenging activity of the PS-MSR is higher than those of both *Cordyceps sinensis* polysaccharides (IC_{50} of 1.23 mg/mL)[47] and *O. sobolifera* polysaccharides (IC_{50} of 0.97 mg/

https://doi.org/10.1021/acsomega.2c05779
ACS Omega 2022, 7, 47923−47932

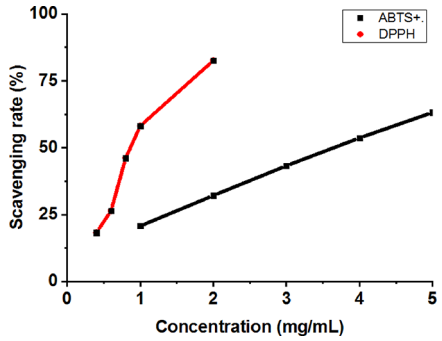

Figure 5. *In vitro* antioxidant activity of PS-MSR. Scavenging effects of PS-MSR on the DPPH radical and $ABTS^{+\cdot}$ radical.

mL).[46] Moreover, the found DPPH radical scavenging activity of the PS-MSR is higher than those of both the *Ganoderma lucidum* polysaccharides.[48] The mentioned pieces of evidence suggest a great antioxidant capability of the PS-MSR sample toward antioxidant properties of rich D-fructose-containing polysaccharides, which has been explored from the roots of *M. smilacifolium* for the first time.

4. CONCLUSIONS

In summary, a novel and rich D-Fruc*f* heteropolysaccharide has been isolated and identified from the *M. smilacifolium* roots. The molecular weight of PS-MSR is found to be 1.88×10^4 Da and is composed of two main sugars, D-glucose and D-fructose, in the backbone. Decoding the structural feature of PS-MSR through the combination of various structural characterization methods unveils the repeating unit of the separated polysaccharide, which is $[\rightarrow 3)$-α-D-Glc*p*-$(1 \rightarrow 3)$-β-D-Fruc*f*-$(2 \rightarrow 3))$-β-D-Fruc*f*-$2 \rightarrow 3)$-$)$-β-D-Fruc*f*-β-$(2\rightarrow]_n$. Impressively, the achieved PS-MSR sample exhibits significant antioxidant activity *in vitro*. The explored polysaccharide can open a new chapter for the applications of *M. smilacifolium*-extracted polysaccharide as a potential antioxidant-based material for biomedical applications at a larger scale.

■ ASSOCIATED CONTENT

Supporting Information

The Supporting Information is available free of charge at https://pubs.acs.org/doi/10.1021/acsomega.2c05779.

GC−MS chromatogram of the PS-MSR sample after methylation, IC_{50} values obtained from ABTS radical scavenging activity of reported polyscaccharides, and IC_{50} values obtained from DPPH radical scavenging activity of reported polyscaccharides (PDF)

■ AUTHOR INFORMATION

Corresponding Authors

Trung Hieu Le − *Hue University of Sciences, Hue University, Hue 530000, Vietnam;* orcid.org/0000-0003-0045-1090; Email: lthieu@hueuni.edu.vn

Chinh Chien Nguyen − *Institute of Research and Development, Duy Tan University, Da Nang 550000, Vietnam; Faculty of Environmental and Chemical Engineering, Duy Tan University, Da Nang 550000, Vietnam;* orcid.org/0000-0002-2852-1102; Email: nguyenchinhchien@duytan.edu.vn

Quyet Van Le − *Department of Materials Science and Engineering, Institute of Green Manufacturing Technology, Korea University, Seoul 02841, Republic of Korea;* Email: quyetbk88@korea.ac.kr

Authors

Lam Son Le − *Hue University of Sciences, Hue University, Hue 530000, Vietnam*

Dang Giang Chau Nguyen − *Hue University of Sciences, Hue University, Hue 530000, Vietnam*

Thi Van Thi Tran − *Hue University of Sciences, Hue University, Hue 530000, Vietnam*

Xuan Anh Vu Ho − *Hue University of Sciences, Hue University, Hue 530000, Vietnam*

Thanh Minh Tran − *Hue University of Sciences, Hue University, Hue 530000, Vietnam*

Minh Nhung Nguyen − *Department of Science and Technology of Thua Thien Hue, Technical Center for Quality Measurement Standards, Hue City 530000, Vietnam*

Viet Thang Nguyen − *Hue University of Sciences, Hue University, Hue 530000, Vietnam*

Thuy Trang Le − *Hue University of Sciences, Hue University, Hue 530000, Vietnam*

Thi Hong Chuong Nguyen − *Institute of Research and Development, Duy Tan University, Da Nang 550000, Vietnam; Faculty of Environmental and Chemical Engineering, Duy Tan University, Da Nang 550000, Vietnam*

Complete contact information is available at: https://pubs.acs.org/10.1021/acsomega.2c05779

Author Contributions

Conceptualization: T.H.L., L.S.L., D.G.C.N., T.V.T.T., X.A.V.H., T.M.T., M.N.N., V.T.N., T.T.L., T.H.C.N., and C.C.N.; formal analysis: T.H.L.; writing−original draft preparation: T.H.L. and T.H.C.N.; writing−review and editing: T.H.L., T.H.C.N., C.C.N., and Q.V.L.; visualization: D.G.C.N., T.V.T.T., X.A.V.H., and C.C.N.; and supervision: T.H.L., C.C.N., and Q.V.L. All authors have read and agreed to the published version of the manuscript.

Funding

The authors acknowledge the support of Hue University under the Core Research Group Program, grant no. NCM.DHH.2020.05. This research was funded by the Vietnamese Ministry of Education and Training under project number B2022-DHH-12 (T.H.L.).

Notes

The authors declare no competing financial interest.

■ REFERENCES

(1) Barclay, T. G.; Day, C. M.; Petrovsky, N.; Garg, S. Review of polysaccharide particle-based functional drug delivery. *Carbohydr. Polym.* **2019**, *221*, 94−112.

(2) Tzianabos, A. O. Polysaccharide immunomodulators as therapeutic agents: structural aspects and biologic function. *Clin. Microbiol. Rev.* **2000**, *13*, 523−533.

(3) Leung, M.; Liu, C.; Koon, J.; Fung, K. Polysaccharide biological response modifiers. *Immunol. Lett.* **2006**, *105*, 101−114.

(4) Liu, Y.; Sun, Y.; Huang, G. Preparation and antioxidant activities of important traditional plant polysaccharides. *Int. J. Biol. Macromol.* **2018**, *111*, 780−786.

(5) Yan, J.; Zhu, L.; Qu, Y.; Qu, X.; Mu, M.; Zhang, M.; Muneer, G.; Zhou, Y.; Sun, L. Analyses of active antioxidant polysaccharides from four edible mushrooms. *Int. J. Biol. Macromol.* **2019**, *123*, 945−956.

(6) Fan, Y.; He, X.; Zhou, S.; Luo, A.; He, T.; Chun, Z. Composition analysis and antioxidant activity of polysaccharide from Dendrobium denneanum. *Int. J. Biol. Macromol.* **2009**, *45*, 169−173.

(7) Dore, C. M. P. G.; Alves, M. G. C. F.; Santos, N. D.; Cruz, A. K. M.; Câmara, R. B. G.; Castro, A. J. G.; Alves, L. G.; Nader, H. B.; Leite, E. L. Antiangiogenic activity and direct antitumor effect from a sulfated polysaccharide isolated from seaweed. *Microvasc. Res.* **2013**, *88*, 12−18.
(8) Chen, L.; Huang, G. The antiviral activity of polysaccharides and their derivatives. *Int. J. Biol. Macromol.* **2018**, *115*, 77−82.
(9) Cao, Y.-G.; Hao, Y.; Li, Z.-H.; Liu, S.-T.; Wang, L.-X. Antiviral activity of polysaccharide extract from Laminaria japonica against respiratory syncytial virus. *Biomed. Pharmacother.* **2016**, *84*, 1705−1710.
(10) Wu, J.; Gao, W.; Song, Z.; Xiong, Q.; Xu, Y.; Han, Y.; Yuan, J.; Zhang, R.; Cheng, Y.; Fang, J.; Li, W.; Wang, Q. Anticancer activity of polysaccharide from Glehnia littoralis on human lung cancer cell line A549. *Int. J. Biol. Macromol.* **2018**, *106*, 464−472.
(11) Chen, H.; Zhang, M.; Xie, B. Components and antioxidant activity of polysaccharide conjugate from green tea. *Food Chem.* **2005**, *90*, 17−21.
(12) Hui, Y.; Jun-Li, H.; Chuang, W. Anti-oxidation and anti-aging activity of polysaccharide from Malus micromalus Makino fruit wine. *Int. J. Biol. Macromol.* **2019**, *121*, 1203−1212.
(13) Yuan, Y.; Zhou, J.; Zheng, Y.; Xu, Z.; Li, Y.; Zhou, S.; Zhang, C. Beneficial effects of polysaccharide-rich extracts from Apocynum venetum leaves on hypoglycemic and gut microbiota in type 2 diabetic mice. *Biomed. Pharmacother.* **2020**, *127*, No. 110182.
(14) Ding, X.; Hou, Y.; Hou, W. Structure feature and antitumor activity of a novel polysaccharide isolated from Lactarius deliciosus Gray. *Carbohydr. Polym.* **2012**, *89*, 397−402.
(15) Lin, T.; Liu, Y.; Lai, C.; Yang, T.; Xie, J.; Zhang, Y. The effect of ultrasound assisted extraction on structural composition, antioxidant activity and immunoregulation of polysaccharides from Ziziphus jujuba Mill var. spinosa seeds. *Ind. Crops Prod.* **2018**, *125*, 150−159.
(16) Jiang, J.; Kong, F.; Li, N.; Zhang, D.; Yan, C.; Lv, H. Purification, structural characterization and in vitro antioxidant activity of a novel polysaccharide from Boshuzhi. *Carbohydr. Polym.* **2016**, *147*, 365−371.
(17) Gong, P.; Wang, S.; Liu, M.; Chen, F.; Yang, W.; Chang, X.; Liu, N.; Zhao, Y.; Wang, J.; Chen, X. Extraction methods, chemical characterizations and biological activities of mushroom polysaccharides: A mini-review. *Carbohydr. Res.* **2020**, *494*, No. 108037.
(18) Maity, P.; Sen, I. K.; Chakraborty, I.; Mondal, S.; Bar, H.; Bhanja, S. K.; Mandal, S.; Maity, G. N. Biologically active polysaccharide from edible mushrooms: A review. *Int. J. Biol. Macromol.* **2021**, *172*, 408−417.
(19) Yu, Y.; Shen, M.; Song, Q.; Xie, J. Biological activities and pharmaceutical applications of polysaccharide from natural resources: A review. *Carbohydr. Polym.* **2018**, *183*, 91−101.
(20) Liu, Y.; Duan, X.; Duan, S.; Li, C.; Hu, B.; Liu, A.; Wu, Y.; Wu, H.; Chen, H.; Wu, W. Effects of in vitro digestion and fecal fermentation on the stability and metabolic behavior of polysaccharides from Craterellus cornucopioides. *Food Funct.* **2020**, *11*, 6899−6910.
(21) Tang, Q.; Huang, G. Improving method, properties and application of polysaccharide as emulsifier. *Food Chem.* **2021**, No. 131937.
(22) Vuong, N. Q.; Van Chien, V.; Hue, N. T.; Hang, P. T.; Van Hieu, T.; Nhiem, N. X.; Cuong, P. V. CHEMICAL CONSTITUENTS FROM THE ROOTS OF MYXOPYRUM SMILACIFOLIUM. *Vietnam J. Sci. Technol.* **2021**, *59*, 498−498.
(23) Sudharmini, D.; Nair, A. S. Antimicrobial studies of triterpenoid fractions from Myxopyrum smilacifolium Blume. *Ethnobot. leafl.* **2008**, *2008*, 123.
(24) Peeriga, R.; Bonnth, C. K. Pharmacognostical Investigation and Preliminary Phytochemical Screening of Leaves of Myxopyrum Smilacifolium B. *Pharmacogn. J.* **2016**, *8*, 159.
(25) Praveen, R.; Ashalatha, S. Study on cytotoxic effect of root and callus extracts of Myxopyrum smilacifolium Blume. *Int. J. Pharm. Sci. Drug Res.* **2015**, *7*, 345−348.
(26) Praveen, R.; Nair, A. Comparative Study on the Antimicrobial Efficacy of Methanolic Extract of Root, Callus and Fruit Extracts of Myxopyrum smilacifolium Blume. *Int. J. Appl. Sci. Biotechnol.* **2015**, *2*, 521−524.
(27) Tran, T. V. T.; Ho, X. A. V.; Le, L. S.; Le, T. H.; Nguyen, T. H. C.; Nguyen, C. C.; Kim, S. Y.; Van Le, Q. Chemical structure of a novel heteroglycan polysaccharide isolated from the biomass of Ophiocordyceps Sobolifera. *J. Mol. Struct.* **2021**, *1232*, No. 129986.
(28) Staub, A. Removeal of protein-Sevag method. *Methods Carbohydr. Chem.* **1965**, *5*, 5−6.
(29) Dubois, M.; Gilles, K. A.; Hamilton, J. K.; Rebers, P. T.; Smith, F. Colorimetric method for determination of sugars and related substances. *Anal. Chem.* **1956**, *28*, 350−356.
(30) Wang, K.; Li, W.; Rui, X.; Chen, X.; Jiang, M.; Dong, M. Characterization of a novel exopolysaccharide with antitumor activity from Lactobacillus plantarum 70810. *Int. J. Biol. Macromol.* **2014**, *63*, 133−139.
(31) Do, T. B. T.; Tran, B. K.; Tran, T. V. T.; Le, T. H.; Cnockaert, M.; Vandamme, P.; Nguyen, T. H. C.; Nguyen, C. C.; Hong, S. H.; Kim, S. Y. Decoding the Capability of Lactobacillus plantarum W1 Isolated from Soybean Whey in Producing an Exopolysaccharide. *ACS Omega* **2020**, *5*, 33387−33394.
(32) Wang, K.; Li, W.; Rui, X.; Chen, X.; Jiang, M.; Dong, M. Structural characterization and bioactivity of released exopolysaccharides from Lactobacillus plantarum 70810. *Int. J. Biol. Macromol.* **2014**, *67*, 71−78.
(33) Li, Q.-Z.; Wu, D.; Zhou, S.; Liu, Y.-F.; Li, Z.-p.; Feng, J.; Yang, Y. Structure elucidation of a bioactive polysaccharide from fruiting bodies of Hericium erinaceus in different maturation stages. *Carbohydr. Polym.* **2016**, *144*, 196−204.
(34) Nagar, S.; Lakhera, A. K.; Kumar, V. Upgrading Methylation Method for Structural Studies of Polysaccharides: Case Analysis of a Bioactive Polysaccharide from Acacia tortilis. *J. Biol. Act. Prod. Nat.* **2020**, *10*, 70−85.
(35) Chen, J.; Pang, W.; Kan, Y.; Zhao, L.; He, Z.; Shi, W.; Yan, B.; Chen, H.; Hu, J. Structure of a pectic polysaccharide from Pseudostellaria heterophylla and stimulating insulin secretion of INS-1 cell and distributing in rats by oral. *Int. J. Biol. Macromol.* **2018**, *106*, 456−463.
(36) Ciucanu, I.; Kerek, F. A simple and rapid method for the permethylation of carbohydrates. *Carbohydr. Res.* **1984**, *131*, 209−217.
(37) Ren, J.; Hou, C.; Shi, C.; Lin, Z.; Liao, W.; Yuan, E. A polysaccharide isolated and purified from Platycladus orientalis (L.) Franco leaves, characterization, bioactivity and its regulation on macrophage polarization. *Carbohydr. Res.* **2019**, *213*, 276−285.
(38) Nair, V. D.; Panneerselvam, R.; Gopi, R. Studies on methanolic extract of Rauvolfia species from Southern Western Ghats of India−In vitro antioxidant properties, characterisation of nutrients and phytochemicals. *Ind. Crops Prod.*. **2012**, *39*, 17−25.
(39) Jayaprakasha, G.; Selvi, T.; Sakariah, K. Antibacterial and antioxidant activities of grape (Vitis vinifera) seed extracts. *Food Res. Int.* **2003**, *36*, 117−122.
(40) Re, R.; Pellegrini, N.; Proteggente, A.; Pannala, A.; Yang, M.; Rice-Evans, C. Antioxidant activity applying an improved ABTS radical cation decolorization assay. *Free Radical Biol. Med.* **1999**, *26*, 1231−1237.
(41) Wong, S. P.; Leong, L. P.; Koh, J. H. W. Antioxidant activities of aqueous extracts of selected plants. *Food Chem.* **2006**, *99*, 775−783.
(42) Liang, Z.; Yi, Y.; Guo, Y.; Wang, R.; Hu, Q.; Xiong, X. Chemical characterization and antitumor activities of polysaccharide extracted from Ganoderma lucidum. *Int. J. Mol. Sci.* **2014**, *15*, 9103−9116.
(43) Wu, F.; Yan, H.; Ma, X.; Jia, J.; Zhang, G.; Guo, X.; Gui, Z. Comparison of the structural characterization and biological activity of acidic polysaccharides from Cordyceps militaris cultured with different media. *World J. Microbiol. Biotechnol.* **2012**, *28*, 2029−2038.
(44) Kacurakova, M.; Capek, P.; Sasinkova, V.; Wellner, N.; Ebringerova, A. FT-IR study of plant cell wall model compounds:

https://doi.org/10.1021/acsomega.2c05779
ACS Omega 2022, 7, 47923−47932

pectic polysaccharides and hemicelluloses. *Carbohydr. Polym.* **2000**, *43*, 195−203.
(45) Wang, Y.; Wei, X.; Wang, F.; Xu, J.; Tang, X.; Li, N. Structural characterization and antioxidant activity of polysaccharide from ginger. *Int. J. Biol. Macromol.* **2018**, *111*, 862−869.
(46) Le, T. H.; Thi Tran, T. V.; Tran, V. K.; Vu Ho, X. A.; Tran, T. M.; Chau Nguyen, D. G.; Chuong Nguyen, T. H.; Varma, R. S.; Trinh, T. K.; Ho, T.-T. Structural Characterization of Mannoglucan Isolated from Ophiocordyceps sobolifera and Its Antioxidant Activities. *ACS Omega* **2022**, *7*, 9397−9405.
(47) Dong, C.-H.; Yao, Y.-J. In vitro evaluation of antioxidant activities of aqueous extracts from natural and cultured mycelia of Cordyceps sinensis. *LWT - Food Sci. Technol.* **2008**, *41*, 669−677.
(48) Zhang, Y.; Feng, Y.; Wang, W.; Jia, L.; Zhang, J.Characterization and hepatoprotections of Ganoderma lucidum Polysaccharides against multiple organ dysfunction syndrome in mice. *Oxid. Med. Cell. Longevity***2021**, *2021*, DOI: 10.1155/2021/9703682.

https://doi.org/10.1021/acsomega.2c05779
ACS Omega 2022, 7, 47923−47932